This is a previous version of the article published in Journal of CO2 Utilization. 2019, 34: 215-230. doi:10.1016/j.jcou.2019.05.005

Optimal Carbon Dioxide and Hydrogen Utilization in Carbon Monoxide Production

Medrano-García, J.D., Ruiz-Femenia, R.* and Caballero, J.A.

Institute of Chemical Process Engineering, University of Alicante, PO 99E-03080 Alicante, Spain

*ruben.ruiz@ua.es

ABSTRACT: Carbon monoxide is the building block of many relevant chemical products. However, the relatively high emissions (1.396 - 2.322 kg CO_2-eq/kg CO) of its synthesis and separation process result in high emitting derivatives. Therefore, reducing CO synthesis emissions is the first step towards more sustainable end products. In order to tackle this problem, we propose a carbon monoxide synthesis and purification superstructure. We perform multi-objective optimizations minimizing the cost and emission of the final CO product across several case scenarios. Results show that the minimum cost solutions are achieved using partial oxidation of methane (POX) as the syngas synthesis process and cryogenic distillation as the CO separation technology. Emissions can be decreased using dry methane reforming (DMR) and pressure swing adsorption (PSA) but costs increase dramatically. Optimal H_2 utilization results in a reverse water gas shift (RWGS) reactor where CO_2 is consumed to produce additional CO. Off-gas valorization is key to further reducing the synthesis cost and emissions.

KEYWORDS: *CO_2 utilization, synthesis gas, methane reforming, carbon monoxide production, hydrogen management, superstructure decision making, multi-objective optimization*

ABBREVIATIONS

ATR	Auto thermal reforming

CCS	Carbon Capture and Storage
BR	Bi-reforming
CO_2-eq	Carbon dioxide equivalent
CR	Combined reforming
DMR	Dry methane reforming
GDP	Generalized Disjunctive Programming
GWP	Global Warming Potential
HI	Heat integration
POX	Partial oxidation
PSA	Pressure swing adsorption
RWGS	Reverse water gas shift
SMR	Steam methane reforming
STAC	Specific total annualized cost
TR	Tri-reforming
WGS	Water gas shift

NOMENCLATURE

Indices

b	bypass: B = {bypass1, bypass2, bypass3}
c	cold stream: $C = \left\{ (c)_{c=1}^{c=19} \right\}$

crwgs Set relation between RWGS reactor *rwgs* and cold stream *c*: $CRWGS_{rwgs,c} = \left\{ \begin{matrix} (1,c12),(1,c13),(2,c14),(2,c15), \\ (3,c16),(3,c17),(4,c18),(4,c19) \end{matrix} \right\}$

csyn Set relation between syngas technology *syn* and cold stream *c*: $CSYN_{syn,c} = \left\{ \begin{matrix} (SMR,c1),(SMR,c2),(POX,c3),(ATR,c4),(CR,c5),(CR,c6), \\ (DMR,c7),(DMR,c8),(BR,c9),(BR,c10),(TR,c11) \end{matrix} \right\}$

d side draw: D = {water, CO_2, H_2 pure, H_2-rich, CO}

e side draw end use: E = {syngas synthesis, recycle, RWGS reactor, fuel cell, fuel gas, byproduct, storage, waste}

h hot stream: $H = \left\{ (h)_{h=1}^{h=13} \right\}$

hrwgs Set relation between RWGS reactor *rwgs* and hot stream *h*: $HRWGS_{rwgs,h} = \left\{ (1,h10),(2,h11),(3,h12),(4,h13) \right\}$

hsyn Set relation between RWGS reactor *rwgs* and hot stream *h*: $HSYN_{syn,h} = \left\{ \begin{matrix} (SMR,h1),(POX,h2),(ATR,h3),(CR,h4), \\ (CR,h5),(DMR,h6),(BR,h7),(TR,h8),(TR,h9) \end{matrix} \right\}$

i process units: I = {syngas synthesis, flash separator, CO_2 absorber1, PSA H_2, cryogenic distillation, PSA CO, CO absorber, CO_2 absorber2, fuel cell, RWGS reactor}

j components: J = {methane, steam/water, O_2, CO_2, CO, H_2}

j' component: J' = { $j' \in J$: j' is the reference component of process unit i } : $\forall i \in I$

k unit types: K = { reformer reactor, compressor, exchanger/heater/cooler, vessel, fuel cell}

og off-gas H_2/CO ratio: OG = {0, 1, 1.5, 2, 2.5, 100}

rwgs reverse water gas shift reactor: $RWGS_i$ = {1, 2, 3, 4} : i = {RWGS reactor}

s process sections: S = {syngas synthesis, separation, RWGS reactor}

st heat integration stage: $ST = \left\{ (st)_{st=1}^{st=58} \right\}$

syn syngas technologies: SYN_i = {SMR, POX, ATR, CR, DMR, BR, TR} : i = {syngas synthesis}

u utilities: U = {natural gas, cooling water, power}

Parameters

a_{iu} Utility u required by process unit i [kW]

AF	Annualization factor
b_i	Additional utilities required by process unit i [various units]
B_k^1	Bare module parameter 1 of unit type k
B_k^2	Bare module parameter 2 of unit type k
c_{ik}^f	Fixed cost parameter of unit type k in process unit i [$]
c_{ik}^v	Variable cost parameter of unit type k in process unit i [$/capacity units]
$F_{\max}$	Maximum allowed molar flow [kmol/h]
F_k^M	Material factor of unit type k
F_k^P	Pressure factor of unit type k
G_j	Mole of CO_2 produced by the complete combustion per mole of component j with air [kmol CO_2/kmol j]
M_{CO_2}	Molar mass of CO_2 [kg CO_2/kmol CO_2]
σ_j	Cost of component j [$/kmol j]
ΔH_j^c	Enthalpy of combustion of component j [kJ/kmol j]
ΔT_{st}	Temperature difference between stage st and $st+1$
ϕ_{ijd}	Fraction separated of component j in process unit i and side draw d
φ_u	Cost contribution of utility u [$/kW]
λ_j	Emission of component j [kg CO_2-eq/kmol j]
η_c	Fuel gas combustion efficiency
θ_u	Emission contribution of utility u [kg CO_2-eq/kW]
ψ_i	Emission contribution of additional utilities [kg CO_2-eq/various units]
ω_i	Cost contribution of additional utilities [$/various units]
Variables	
cap_i	Capital cost of process unit i [$]
$cost_{og}$	Off-gas valorization associated revenue [$/kg]
$emission_i$	Emission of process unit i [kg CO_2-eq/h]

$emission_{og}$	Off-gas valorization associated abated emission [kg CO_2-eq/kg]
$emission^{fg}$	Emission related to fuel gas combustion [kg CO_2-eq/h]
F_{ijde}	Molar flow of component j in side draw d end use e from process unit i [kmol/h]
$F_{CO_2}^{ex}$	Additional CO_2 molar flow that enters the system [kmol/h]
F_j^{fg}	Fuel gas molar flow of component j [kmol/h]
F_{bj}^{in}	Inlet bypass b molar flow of component j [kmol/h]
F_{bj}^{out}	Outlet bypass b molar flow of component j [kmol/h]
F_{ij}^{in}	Inlet process unit i molar flow of component j [kmol/h]
F_{ij}^{out}	Outlet process unit i molar flow of component j [kmol/h]
$F_j^{product}$	Product molar flow of component j [kmol/h]
FCp_{stc}	Product of the molar flow and heat capacity of cold stream c in stage st per kmol/h of component j' [kW·ºC·h/kmol j']
FCp_{sth}	Product of the molar flow and heat capacity of hot stream h in stage st per kmol/h of component j' [kW·ºC·h/kmol j']
H_2/CO	Off-gas H_2/CO molar ratio
op_i	Operating cost of process unit i [$/h]
Q_{cold}	Total cold services required by the system [kW]
Q_i	Hot services required by process unit i [kW]
Q_i^{fg}	Hot services provided to process unit i by fuel gas combustion [kW]
Q_{hot}	Total hot services required by the system [kW]
q_{hot}	Total externally supplied hot services required by the system [kW]
R_{st}	Residual heat that leaves stage st [kW]
raw_j	Raw material molar flow of component j [kmol/h]
y_i	Binary variables associated to the existence of process unit i

1. Introduction

Carbon monoxide is a precursor of many important chemical products (Figure 1). It is most commonly obtained through synthesis gas (syngas) separation, which is mainly an H_2/CO mixture, although it can also contain unreacted methane and unseparated carbon dioxide [1]. Hence, this process produces an excess gas byproduct which is usually hydrogen-rich. This off-gas is often used as fuel within the syngas generation and separation section or in downstream applications, although it can also serve as a raw material of other products since it contains valuable hydrogen.

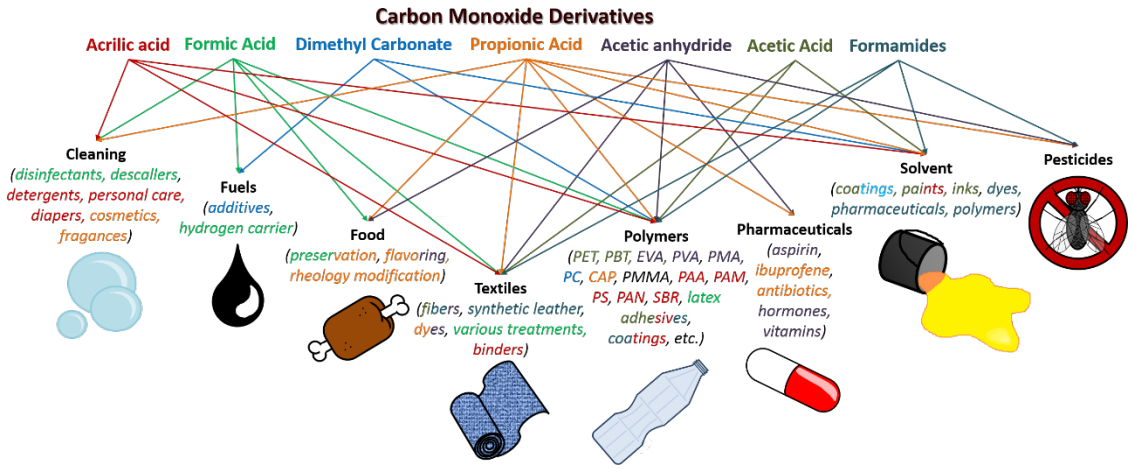

Figure 1. Carbon monoxide main derivatives and applications [2–9]

The synthesis and separation of carbon monoxide has a more than appreciable carbon footprint. The whole process emits approximately from 1.396 to 2.322 kg of carbon dioxide equivalent (kg CO_2-eq) per kg of CO [10]. Therefore, due to the importance of the gas, achieving a reduction of these manufacture emissions may contribute to mitigate the environmental burden.

In a previous work [11], we studied syngas generation and ratio adjustment for several compositions and product pressures. The most remarkable result, at least from an environmental point of view, was that with an H_2/CO ratio of one and low product

pressures, the production of this syngas can consume more CO_2 than it emits both directly and indirectly, down to a minimum value of about –0.2 kg CO_2-eq/kg syngas. This result is directly tied to the need of hydrogen: the less hydrogen required, the less costly and less emitting the synthesis is. According to these results, a further reduction of the H_2/CO ratio could lead to an even higher CO_2 utilization process. Hence, completely removing H_2 from syngas in order to produce pure CO may result in an interesting case of study. We propose a process superstructure in which several syngas synthesis processes, H_2, CO and CO_2 separation units and different off-gas utilization alternatives (fuel gas, fuel cell, Reverse Water Gas Shift reaction) are included. The aim of this superstructure is to find the optimal configuration that minimizes the cost ($/kg CO) and/or the emission (kg CO_2-eq/kg CO) by using classic, CO_2-consuming and more environmentally friendly technologies.

The superstructure is modelled using the Generalized Disjunctive Programming (GDP) and the resulting disjunctions are transformed into algebraic equations through the Hull Reformulation [12]. We tackle this optimization problem solving the resulting Mixed-Integer Non-Linear Program (MINLP) model as a multi-objective optimization problem using the epsilon constraint method [13], minimizing the environmental (GWP) and economic (Specific Total Annualized Cost, STAC) indicators. Results show that the byproduct management is the key to achieve a great reduction both in cost and emissions of the synthesis process.

2. Methods and models

The proposed process superstructure is shown in Figure 2. Methane and the selected reformer agents enter one of the possible syngas synthesis processes. Then, water is removed via condensation, followed by the possibility of removing CO_2 in an amine

absorption process. A Presure Swing Adsorption (PSA) unit may be used to remove H_2 from the resulting stream, or it can simply advance to the CO separation section, where cryogenic distillation, absorption, or PSA can be used for the task. Finally, the product CO stream can be subjected to a further CO_2 removal if needed. Hydrogen rich and off-gas streams resulting from the separation technologies are given the possibility of being recycled, used as fuel (combustion or in a fuel cell) or become a byproduct stream for utilization in a subsequent synthesis. A more in depth analysis of Figure 2 is given in the following subsections.

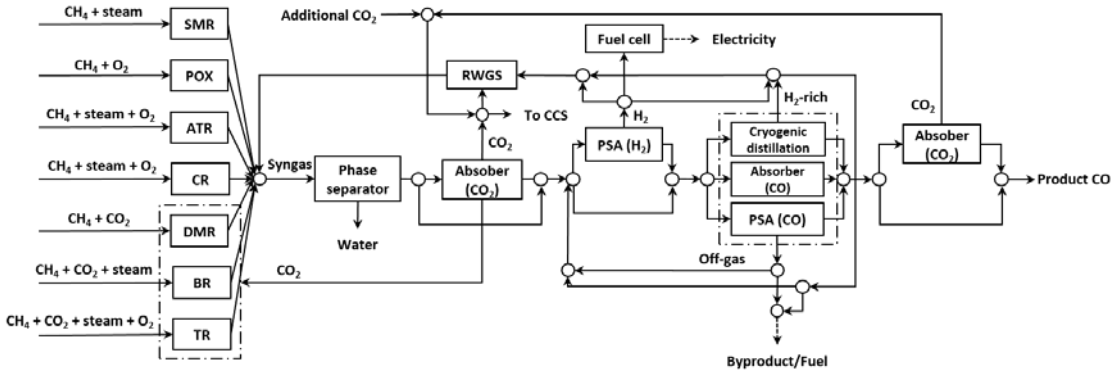

Figure 2. Proposed carbon monoxide synthesis and separation superstructure

2.1.Synthesis gas production

Carbon monoxide can be produced by methane reforming syngas synthesis and its subsequent separation [1,14]. The synthesis can be carried out by several technologies. Steam methane reforming (SMR) uses steam as reforming agent in an endothermic reaction that produces high hydrogen content syngas [15,16]. This is the most used worldwide tehnology, especially when hydrogen is desired as the main or secondary product [17]. Non-catalitic partial oxidation (POX) uses oxygen as reforming agent in a high enxothermic reaction that can reach over 1200 ºC [18], and its catalytic version, auto-thermal reforming (ATR), uses a mixture of oxygen and steam in an also overall

exothermic process [17,19]. These two technologies are the most used after SMR, especially when syngas with low to medium hydrogen content is the main sought product [20,21]. The fourth techonology is combined reforming (CR), which consists in an SMR followed by an ATR reformer reactor [22]. The so called dry methane reforming (DMR) uses CO_2 as the sole reforming agent in order to produce a low hydrogen content syngas in a highly endothermic energy intensive reaction [20,21,23]. The particularity of this process resides in its capability of net consuming CO_2 in the production of low pressure and H_2/CO ratios syngas [11]. Bi-reforming consists in the addition of CO_2 to the SMR reaction [22]. This change reduces the hydrogen content in the product but allows for an easier syngas composition adjustment, in addition to consuming CO_2 in the process [17]. Finally, tri-reforming uses all three reforming agents (steam, oxygen and CO_2) so as to produce syngas with an H_2/CO ratio below two [24,25]. The selected process for CO production is largely dependent on a company's own technologies and licenses [26], although POX, ATR and SMR are usually the preferred choices [20,27].

These processes were simulated in Aspen HYSYS v9.0 using the most common feed ratios and operating pressures and temperatures found in the bibliography. From the simulations, we propose linear models addressing raw material and utility requirements, conversion and capital costs. These models as well as a more detailed information on the simulations and operating parameters can be found in [11].

2.2.Carbon monoxide separation

Separation of carbon monoxide is mainly carried out using three different technologies [14,28]: cryogenic distillation, chemical absorption (COSORB) and pressure swing adsorption (PSA). Cryogenic distillation is the most widley used [29], while absorption and PSA are more suitable when N_2 is present in the mixture [30]. Carbon monoxide

purities and recoveries, as well as the cost and emission per mass unit of CO separated are shown in Table 1.

Table 1. Main carbon monoxide separation technologies and characteristics [28].

	Cryogenic distillation	**COSORB**	**PSA**
CO Purity [%]	97 - 99 [30,31]	99	99
CO Recovery [%]	90	99	90
Cost [$/ton CO]	71 [29]	200 [32]	140 [32]
GWP [kg CO_2-eq/kg CO]	0.587 [33]	0.190 [32]	0.094 [32]*

* 1.4 bar inlet pressure

2.3. Hydrogen optimal usage

2.3.1. Fuel gas production for energy generation

The continuous availability of hydrogen combined with its clean combustion makes it an excellent candidate to be used as fuel in the syngas synthesis process and the following downstream applications. Recycling the fuel gas reduces natural gas demand, and thus the cost and—most importantly—the emission of heating. The energy produced by the fuel gas is calculated as:

$$\sum_i Q_i^{fg} = \sum_j \Delta H_j^c F_j^{fg} \eta_c \quad (1)$$

Where Q_i^{fg} (kW) is the energy produced by combustion of the fuel gas which is sent to process unit i, ΔH_j^c is the enthalpy of combustion of component j (Table 2), F_j^{fg} is the fuel gas molar flow of component j (kmol/s) and η_c is the efficiency of the combustion,

assumed at 0.8. The total hot services energy demand of the system that has to be externally supplied, q_{hot}, is calculated using Eq.(2) and Eq.(3), subjected to Eq.(4):

$$Q_{hot} = \sum_i Q_i \tag{2}$$

$$q_{hot} = \sum_i \left(Q_i - Q_i^{fg} \right) \quad \forall i \in I \tag{3}$$

$$Q_i - Q_i^{fg} \geq 0 \quad \forall i \in I \tag{4}$$

where Q_i is the hot services energy demand of process unit i and Q_{hot} is the total energy demand (hot services) of the system, both in kW. If part of the energy is unused by the system, it is sold assuming the same price if it was produced by burning natural gas (9.237 \$/MWh [34]). On the other hand, its CO_2 emissions are calculated assuming total combustion of the gas minus the avoided emissions of the same quantity of natural gas based energy would produce (212.2 kg CO_2-eq/MWh [10]).

Unreacted methane and unseparated carbon monoxide and dioxide can be part of the fuel gas, which makes its combustion not completely emission free. Total combustion of the fuel gas is assumed when computing the emission:

$$emission^{fg} = \sum_j F_j^{fg} G_j M_{CO_2} \tag{5}$$

where G_j is the molar production of CO_2 after combustion with air of component j (Table 2), M_{CO_2} is the molar mass of CO_2 (44 kg/kmol) and $emission^{fg}$ is the mass flow of CO_2 produced by combustion of the fuel gas (kg/s).

Table 2. Combustion enthalpies, molar production of CO_2 and cost of the most prominent fuel gas components in this system.

	H_2	**CH_4**	**CO**	**CO_2**
ΔH^c_j [kJ/kmol]	241814	802518	283200	-
Cost [$/MWh]	-	9.237 [34]	-	-
G_j [kmol CO_2/kmol *j*]	-	1	1	1

2.3.2. Off-gas production

The production of an off-gas byproduct is an alternative to the fuel gas route. This approach is interesting when downstream applications require hydrogen or syngas (obtained by leaving unseparated CO) in subsequent synthesis. Example of this are formic acid [5], acetic acid [7] or dimethyl carbonate synthesis [4]. Since this gas is a byproduct, the emission of its components is not included in the environmental indicator save for the carbon dioxide. A CO_2 absorber is assumed to remove 96 % of the gas from the stream with a cost of 43.06 $/ton of CO_2 [35]. The absorber is needed to avoid a CO_2 "leak" through the off-gas, since omitting its contribution would derive in the system removing the maximum quantity possible through the byproduct. Regardless, the option of using part of this off-gas to fuel sections of the superstructure remains available. The economic ($cost_{og}$, $/kg) and environmental ($emission_{og}$, kg CO_2-eq/kg) profit associated to the off-gas utilization is computed using the following correlations, which are adjusted using bibliographic and experimental data (Appendix A, Table A. 7):

$$cost_{og} = \begin{cases} 1.58 - 1.436(H_2/CO) & \forall (H_2/CO) \in [0,1] \\ 0.0721 + 0.1673(H_2/CO) - 0.1222(H_2/CO)^2 + 0.02733(H_2/CO)^3 & \forall (H_2/CO) \in (1,2.5) \\ 0.117 + 0.01463(H_2/CO) & \forall (H_2/CO) \in [2.5,10] \\ 1.58 & \forall (H_2/CO) \in (10,\infty) \end{cases}$$

(6)

$$emission_{og} = \begin{cases} 1.859 - 1.261(H_2/CO) & \forall (H_2/CO) \in [0,1] \\ 0.3376(H_2/CO)^3 - 1.469(H_2/CO)^2 + 2.035(H_2/CO) - 0.3043 & \forall (H_2/CO) \in (1,2.5) \\ 0.8399 + 0.01353(H_2/CO) & \forall (H_2/CO) \in [2.5,10] \\ 2.1924 & \forall (H_2/CO) \in (10,\infty) \end{cases}$$

(7)

where H_2/CO is the off-gas molar hydrogen to carbon monoxide ratio.

2.3.3. Reverse water gas shift reaction

The water gas shift reaction (Eq.(8)) consists in the chemical equilibrium of H_2, CO, CO_2 and steam [36]. This exothermic reaction, which produces H_2 and CO_2, is favored at low temperatures, thus making this the most common technique to increase the H_2/CO ratio of syngas by feeding steam to the mixture. However, at high temperatures, the equilibrium is favored in the opposite direction, in the so called reverse water gas shift (RWGS) reaction:

$$CO + H_2O \underset{RWGS}{\overset{WGS}{\rightleftharpoons}} H_2 + CO_2 \quad (8)$$

Under 600 ºC, the methanation reaction takes place simultaneously, and while under 800 ºC, carbon deposition occurs [37]. However, it has been reported [38] that using a specific NiO/silica based catalyst negates these adverse effects, with low NiO charges of 15 % or less providing results in 100 % CO selectivity (*Table 3*).

Table 3. RWGS reaction CO_2 conversion [38].

CO_2 conversion [%]	11.6	45.0	77.6	85.9
T [ºC]	300	350	400	450
P [bar]	1			
H_2/CO [mol/mol]	7			

We perform simulations in Aspen HYSYS v9.0 using the temperatures, pressure, feed ratio and conversions stated in *Table 3*. The results of the simulations (energy requirements) allow us to build linear equations to model the reactor. The related data is contained in the Appendix tables (Table A.4, Table A.5 and Table B.1).

2.3.4. Electricity generation

Renewable electricity by hydrogen reverse electrolysis in a fuel cell is no doubt an efficient and clean energy source. The main inconvenience it presents is hydrogen availability (generation and transport), which usually increases its cost compared to classic fossil fuel electricity [39]. In this particular scenario, since hydrogen is a byproduct of the main synthesis, it could be considered using part of it to produce clean electricity, cutting the need of a renewable hydrogen source. Commercial proton exchange membrane (PEM) fuel cells can produce 1 MW per 750 Nm^3/h H_2 over 99.99 % purity [40]. A PSA unit is installed in order to achieve this purity [41]. Typical PSA unit recovery for hydrogen production is in the range of 70 – 95 % at high purity (>99.999 %) [42,43].

2.4.Mathematical modelling of the superstructure

2.4.1. Carbon monoxide product line

As seen in Figure 2, raw materials enter the chosen syngas synthesis process at the required ratio. Only one process is allowed to be selected per optimization. More details on the modelling of this section can be found in [11]. Then, the syngas product is sent to the separation section. First, a phase separator working at 40 ºC is considered to remove all water contained in the syngas. Next, the option of removing CO_2 (96 % recovery, 43.06 $/ton [35]) is given. We formulate these options using disjunctions, whose general formulation is as follows:

306
$$\begin{bmatrix} Y_i \\ cap_i = \sum_k \left(c_{ik}^f + c_{ik}^v F_{ij'}^{in}\right)\left(B_k^1 + B_k^2 F_k^M F_k^P\right) \\ 0 \le \sum_j F_{ij}^{in} \le F_{\max} \\ 0 \le \sum_j F_{ij}^{out} \le F_{\max} \\ 0 \le \sum_e \sum_d \sum_j F_{ijde} \le F_{\max} \end{bmatrix} \vee \begin{bmatrix} \neg Y_i \\ F_{ij}^{in} = 0 \\ F_{ij}^{out} = 0 \\ F_{ijde} = 0 \\ cap_i = 0 \end{bmatrix} \quad \forall i, j, j' \in I \times J \qquad (9)$$

307 where Y_i is the Boolean variable related to the existence of the unit. If this variable value
308 is "true", the unit exists and the process flows and cost associated to it also do, otherwise,
309 these variables are zero. This disjunction can be reformulated into a set of algebraic
310 equations using a binary variable (y_i) which adopts the values 1 or 0 if the corresponding
311 Boolean variable is true or false, respectively. Since all the equations enclosed in the
312 disjunction are linear, we apply the Hull reformulation [12]. This reformulation is as
313 follows:

314
$$cap_i = \sum_k \left[\left(c_{ik}^f y_i + c_{ik}^v F_{ij'}^{in}\right)\left(B_k^1 + B_k^2 F_k^M F_k^P\right)\right] \quad \forall i, j' \in I \times J \qquad (10)$$

315
$$0 \le \sum_j F_{ij}^{in} \le F_{\max} y_i \quad \forall i \in I \qquad (11)$$

316
$$0 \le \sum_j F_{ij}^{out} \le F_{\max} y_i \quad \forall i \in I \qquad (12)$$

317
$$0 \le \sum_e \sum_d \sum_j F_{ijde} \le F_{\max} y_i \quad \forall i \in I \qquad (13)$$

318 The capital cost of unit i is referred as cap_i (\$/h), while c_{ik}^f and c_{ik}^v are the fixed and
319 variable cost parameters of unit i and equipment type k estimated from linearizations of
320 the models proposed by Turton et. al [44] (Table A.2). F_k^M and F_{ik}^P are the material and
321 pressure factors associated to equipment type k while B_k^1 and B_k^2 are the bare module
322 parameters of said process unit types. $F_{ij'}^{in}$ (kmol/h) is the inlet molar flow of a specific

component j' used for calculating variable costs and emissions, which is different in each unit i and is usually tied to the main separation component of said unit (Table 4). F_{ij}^{in} and F_{ij}^{out} are the inlet and outlet molar flows of component j in unit i (kmol/h), F_{ijde} are component j, unit i, side draw d molar flows sent to end use e in (kmol/h) and $F_{\max}$ is the allowed upper limit of the molar flow (10 kmol/s). In addition to Eqs.(10)-(13), the other common equations needed for modelling the process units are:

$$F_{ij}^{out} = F_{ij}^{in} - \sum_{e}\sum_{d} F_{ijde} \quad \forall i, j \in I \times J \tag{14}$$

$$\sum_{e} F_{ijde} = \phi_{ijd} F_{ij}^{in} \quad \forall i, j, d \in I \times J \times D \tag{15}$$

$$emission_i = \left(\sum_{u} a_{iu}\theta_u + b_i\psi_i \right) F_{ij'}^{in} - Q_i^{fg}\theta_{natural\ gas} \quad \forall i, j' \in I \times J \tag{16}$$

$$op_i = \left(\sum_{u} a_{iu}\varphi_u + b_i\omega_i \right) F_{ij'}^{in} - Q_i^{fg}\varphi_{natural\ gas} \quad \forall i, j' \in I \times J \tag{17}$$

where ϕ_{ijd} is a parameter that fixes the recovery of component j in unit i and side draw d. The parameter a_{iu} (kW/ kmol j') states how much utility u (natural gas, cooling water, electricity) is needed by unit i, θ_u is the equivalent CO_2 emission of utility u (kg CO_2-eq/kW), b_i is a binary parameter that adds additional contributions, like the use of a solvent, to unit i, and ψ_i (kgCO_2-eq/kmol j'), is the input of said contributions to the process emission ($emission_i$, in kgCO_2-eq/h). The operating cost (op_i) makes use of the same a_{iu} and b_i parameters plus their conversion to costs φ_u (\$/kW) and ω_i (\$/kmol j'). These parameters can be found in Appendix A (Table A.3, Table A.4 and Table A.5).

343 *Table 4. Main components and side draws of process unit i.*

Unit *i*	Component *j'*	Side draw *d*
Reformer reactor	Methane	-
Flash separator	Water	Water
CO_2 absorbers	CO_2	CO_2
H_2 PSA	H_2	H_2 pure
Cryogenic distillation	CO	H_2-rich, CO
CO PSA	CO	CO
CO absorber	CO	H_2-rich, CO
Fuel cell	H_2	-
RWGS reactor	CO_2	-

344

345 After the CO_2 absorber, the gas flow encounters a PSA unit that prioritizes H_2 separation.
346 Here, the same situation, where the unit may or may not exist, is found. The modelling of
347 this unit is equivalent to the absorber, using Eq.(10)-(17) along with the appropriate
348 parameters (Table A.2 - Table A.5). In addition, for both, this and the absorber case, the
349 use of a bypass is proposed as an alternative option if the process unit is not selected,
350 although it can still be chosen in case only a fraction of the gas of interest has to be
351 removed:

352 $$F_{bj}^{in} = F_{bj}^{out} \quad \forall b, j \in B \times J \tag{18}$$

353 $$F_{rr,j}^{out} = F_{abs1,j}^{in} + F_{b1,j}^{in} \quad \forall j \in J \tag{19}$$

354 $$F_{abs1,j}^{out} + F_{b1,j}^{out} = F_{psa1,j}^{in} + F_{b2,j}^{in} \quad \forall j \in J \tag{20}$$

355 where F_{bj}^{in} and F_{bj}^{out} are the inlet and outlet molar flows of component j in bypass b.
356 The subscripts rr, $abs1$, $b1$, $psa1$ and $b2$ stand for the reformer reactor, first CO_2

absorber, first bypass, H_2 PSA and second bypass. Note that in cases where a stream division occurs, a composition mass balance has to be included in order to maintain the composition of the original stream. However, in this case, since the absorber/PSA cost, emission and separation only depends on the main component and both streams converge again before entering the next process unit, the composition mass balance can be skipped and thus the associated nonlinearities are avoided.

The stream then arrives at the main CO separation section. The next equation ensures that only one of the separation technologies is selected:

$$y_{psa2} + y_{cd} + y_{absco} \leq 1 \tag{21}$$

where $psa2$, cd and $absco$ stand for the CO PSA, cryogenic distillation and CO absorption units. The mass balance is as follows:

$$F^{out}_{psa1,j} + F^{out}_{b2,j} = F^{in}_{psa2,j} + F^{in}_{cd,j} + F^{in}_{absco,j} \quad \forall j \in J \tag{22}$$

These units are also modelled using Eqs.(10)-(17). Since only one separation unit can exist, there is no real division, hence the composition mass balance is again avoided. Before the obtaining of the product, an additional CO_2 removal step is added in case too much of the gas remains with it. Finally, the product CO is obtained at > 99 % purity as the sum of the CO rich side draws of these units:

$$F^{product}_{j} = F^{CO}_{cd,j} + F^{CO}_{absco,j} + F^{CO}_{psa2,j} \quad \forall j \in J \tag{23}$$

where $F^{product}_{j}$ is the molar flow of the product stream in kmol/h.

2.4.2. Side draw management

The side draws of all these separation units are split or mixed depending on their composition (Table 5). The CO_2 draws obtained in the CO_2 absorbers can be used as a

raw material in the RWGS reactor, any of the CO_2-consuming methane reforming processes or just stored. On the other hand, there are two different H_2 draws: the H_2-rich streams obtained in the cryogenic distillation and CO absorber units and the fuel cell grade almost pure H_2 stream obtained in the first PSA. The fuel cell operates using H_2 exclusively extracted in the first PSA (fuel cell grade H_2 stream). In addition, the remaining H_2 of this stream can enter the RWGS reactor, be used as fuel or become the byproduct. These three options are also available for the H_2-rich streams. Furthermore, the H_2-rich stream can be recycled back just before the first PSA choice, in case additional H_2 has to be recovered. Therefore, the mass balances associated to the end uses of the side draws are as follows:

$$\left(F_{ij}^{in} - F_{ij}^{out}\right)\sum_{j} F_{ijde} = \sum_{j}\left(F_{ij}^{in} - F_{ij}^{out}\right)F_{ijde} \qquad \forall j \in J, \forall (i,d) \in (I \times D') \wedge \forall (d,e) \in (D' \times E') \tag{24}$$

where the relations of unit i and side draw d ($I \times D'$) and side draw d and end use e ($D' \times E'$) are stablished in Table 4 and Table 5.

Table 5. Side draws of the separation units and possible uses

Side draw *d*	**End use *e***
Water	waste
CO_2	syngas synthesis, RWGS reactor, storage
H_2 pure	fuel cell, RWGS reactor, fuel gas, byproduct
H_2-rich	recycle, RWGS reactor, fuel gas, byproduct
CO	product*

*not considered a side draw since the main superstructure flow follows this path

2.4.3. Heat integration

Heat integration (HI) is key in reducing the energetic demand in many chemical processes, and in the case of syngas synthesis, it is particularly important. The high temperatures needed in the synthesis are translated into a high energy demand, while such demand derives into elevated costs and emissions. We integrate HI into the superstructure using the transshipment problem approach [45], which is illustrated in Appendix B (Figure B.1). This method consists in the division of the system hot (h) and cold (c) streams into stages (st) following the stream ordered temperatures (Table B.1). The temperatures of the hot streams are subtracted $\Delta T/2$, while the opposite is done for the cold streams, where ΔT is the minimum temperature difference allowable for any heat transfer, which is set to 10 ºC in this work. Here, each stream exchanges heat in all stages that are included in its temperature range. The total hot utility (Q_{hot}, kW) heat flow the system needs enters on the first stage, while the total cold utility (Q_{cold}, kW) heat flow required by the system leaves the last stage. In addition, a residual heat (R_{st}, kW) leaves stage st and enters stage $st+1$ connecting all stages by their respective energy balances (Eqs. (25)-(27)).

$$\sum_{HSYN_{syn,h}} \left(\Delta T_1 FCp_{1h} F^{in}_{syn,j'}\right) + \sum_{HRWGS_{rwgs,h}} \left(\Delta T_1 FCp_{1h} F^{in}_{rwgs,j'}\right) + Q_{hot} = \sum_{CSYN_{syn,c}} \left(\Delta T_1 FCp_{1c} F^{in}_{syn,j'}\right) + \sum_{CRWGS_{rwgs,c}} \left(\Delta T_1 FCp_{1c} F^{in}_{rwgs,j'}\right) + R_1 \quad \forall j' \in J \tag{25}$$

$$\sum_{HSYN_{syn,h}} \left(\Delta T_{st} FCp_{st,h} F^{in}_{syn,j'}\right) + \sum_{HRWGS_{rwgs,h}} \left(\Delta T_{st} FCp_{st,h} F^{in}_{rwgs,j'}\right) + R_{st-1} = \sum_{CSYN_{syn,c}} \left(\Delta T_{st} FCp_{st,c} F^{in}_{syn,j'}\right) + \sum_{CRWGS_{rwgs,c}} \left(\Delta T_{st} FCp_{st,c} F^{in}_{rwgs,j'}\right) + R_{st} \tag{26}$$
$$\forall j' \in J, \forall st \in ST \setminus \left\{1, |ST|\right\}$$

$$\sum_{HSYN_{syn,h}} \left(\Delta T_{|ST|} FCp_{|ST|h} F^{in}_{syn,j'}\right) + \sum_{HRWGS_{rwgs,h}} \left(\Delta T_{|ST|} FCp_{|ST|h} F^{in}_{rwgs,j'}\right) + R_{|ST|-1} = \sum_{CSYN_{syn,c}} \left(\Delta T_{|ST|} FCp_{|ST|c} F^{in}_{syn,j'}\right) + \sum_{CRWGS_{rwgs,c}} \left(\Delta T_{|ST|} FCp_{|ST|c} F^{in}_{rwgs,j'}\right) + Q_{cold} \quad \forall j' \in J \tag{27}$$

where ΔT_{st} is the temperature increment in stage st, $FCp_{st,h}$ and $FCp_{st,c}$ are the products of the molar flows and heat capacities per kmol/h of component j' (kW·h·ºC/kmol j') of hot stream h and cold stream c located at stage st and $HSYN_{syn,h}$, $CSYN_{syn,c}$, $HRWGS_{rwgs,h}$ and $CRWGS_{rwgs,c}$ are the set relations between syngas synthesis technologies (SYN_i) and RWGS reactor types ($RWGS_i$) and the hot h and cold c streams (Eqs.(28) -(31)).

$$HSYN_{syn,h} = \left\{ \begin{matrix} (SMR,h1),(POX,h2),(ATR,h3),(CR,h4), \\ (CR,h5),(DMR,h6),(BR,h7),(TR,h8),(TR,h9) \end{matrix} \right\} \tag{28}$$

$$CSYN_{syn,c} = \left\{ \begin{matrix} (SMR,c1),(SMR,c2),(POX,c3),(ATR,c4),(CR,c5),(CR,c6), \\ (DMR,c7),(DMR,c8),(BR,c9),(BR,c10),(TR,c11) \end{matrix} \right\} \tag{29}$$

$$HRWGS_{rwgs,h} = \{(1,h10),(2,h11),(3,h12),(4,h13)\} \tag{30}$$

$$CRWGS_{rwgs,c} = \left\{ \begin{matrix} (1,c12),(1,c13),(2,c14),(2,c15), \\ (3,c16),(3,c17),(4,c18),(4,c19) \end{matrix} \right\} \tag{31}$$

2.4.4. Multi-objective optimization

The objective functions selected for this study are the Specific Total Annualized Cost (STAC) and the Global Warming Potential (GWP). The former is calculated as the sum of the annualized capital and operating costs of the process per kg of product CO:

$$STAC = \left(\sum_i \left(AFcap_i + op_i \right) + raw_j \sigma_j \right) \Big/ F^{product}_{CO} \tag{32}$$

$$raw_j = \sum_{syn} F^{in}_{syn,j} \quad \forall j \in J \setminus \{CO_2\} \tag{33}$$

$$raw_{CO_2} = F^{ex}_{CO_2} + \sum_{syn} F^{in}_{syn,CO_2} \tag{34}$$

$$AF = \frac{IR\left(IR+1\right)^{years}}{\left(IR+1\right)^{years}-1} \tag{35}$$

where raw_j (kmol/h) is the raw material molar flow of component j and σ_j ($/kmol) is a parameter for calculating the cost of those raw materials. The variables $F_{syn,j}^{in}$ and $F_{CO_2}^{ex}$ (kmol/h) stand for the inlet molar flow of component j and syngas synthesis technology syn and the additional CO_2 molar flow that can be used in the RWGS reactor. To compute the annualization factor (AF), the horizon time is 8 years and the interest rate (IR) is set to 0.1 [46]. On the other hand, GWP includes the indirect emission of raw material and energy usage, as well as a term regarding the abatement of CO_2 that is consumed in the system:

$$GWP = \left[\begin{array}{l} \sum_{\forall j \in J \setminus \{CO_2\}} \left(raw_j \lambda_j\right) + emission^{fg} + \sum_i emission_i + \\ +M_{CO_2}\left(\sum_{\forall i \in \{abs1, abs2\}} \sum_e \left(F_{ijde}\right) - raw_j \right) \end{array} \right] \Big/ F_{CO}^{product} \tag{36}$$
$$j = \{CO_2\}, d = \{CO_2\}$$

where λ_j is the GWP contribution of the raw materials (kg CO_2-eq/kmol j).

The overall bi-MINLP formulation can be expressed in compact form as follows:

$$\begin{aligned} &\min_{x,y} \{STAC(x,y); -GWP(x,y)\} \\ &s.t. \qquad constraints \end{aligned} \tag{37}$$

where x and y stand for continuous generic variables associated with structural decisions. Solving this problem results in a set of Pareto alternatives that represent the optimal trade-off between the objectives. We used the ε-constraint method [13] to obtain these Pareto solutions by solving a set of instances of the following single-objective problem ($M1$) for different values of the auxiliary parameter ε:

$$(M1) \qquad \begin{aligned} &\min_{x,y}\{STAC\} \\ &s.t. \quad constraints \\ &GWP \le \varepsilon \\ &\underline{\varepsilon} \le \varepsilon \le \overline{\varepsilon} \end{aligned} \tag{38}$$

Where $\underline{\varepsilon}$ and $\overline{\varepsilon}$ denote the lower and upper bounds of ε, which are obtained by individually optimizing each objective. The minimization of the GWP directly results in the value of $\underline{\varepsilon}$, while the minimization of the STAC provides $\overline{\varepsilon}$, since the lowest cost generates the higher emission:

$$(M1a) \qquad \begin{aligned} &(\overline{x},\overline{y}) = \arg\min_{x,y}\{TAC\} \\ &s.t. \quad \text{constraints} \end{aligned} \tag{39}$$

$$(M1b) \qquad \begin{aligned} &\underline{\varepsilon} = \min_{x,y}\{GWP\} \\ &s.t. \quad \text{constraints} \end{aligned} \tag{40}$$

3. Results and discussion

We optimize the superstructure fixing a molar flow value of the product CO of 0.1 kmol/s. According to this, we bound the problem variables using Aspen HYSYS v9.0 simulations as a reference. Initialization is also carried out with these reference values. The model is comprised of 742 equations and 483 variables, 20 of which are binary variables. We used GAMS [47] and the ANTIGONE solver [48] to implement and solve the problem, respectively.

The main results of the multi-objective optimization problem are shown in Figure 3. Results are separated in different cases: a Base Case where a binary cut prevents the fuel cell and RWGS reactor from appearing in the final solution, Case 1 where the fuel cell is free to be selected, Case 2 where the RWGS reactors are available for selection and Case 3 where any feasible combination contained in the superstructure is a valid solution.

Parting from the solutions of each individual case, the byproduct off-gas is then valorized both economically and environmentally in two additional scenarios per case study: its combustion and use as energy and its utilization as syngas outside the boundaries of the system. The valorization as energy considers that it substitutes natural gas combustion, hence, its selling cost is considered the same (9.237 $/MWh [34]). On the other hand, its CO_2 emissions are calculated assuming total combustion of the gas minus the avoided emissions of the same quantity of natural gas based energy would produce (212.2 kg CO_2-eq/MWh [10]). Utilization as hydrogen/syngas is valorized using Eqs.(6)-(7) adjusted from the economic and environmental values of syngas with H_2/CO ratios of 1.0, 1.5, 2.0 and 2.5 in addition to considering the extreme cases where only CO (H_2/CO ratio is zero) or H_2 is produced (H_2/CO assumed 100 or more) (Table A. 7).

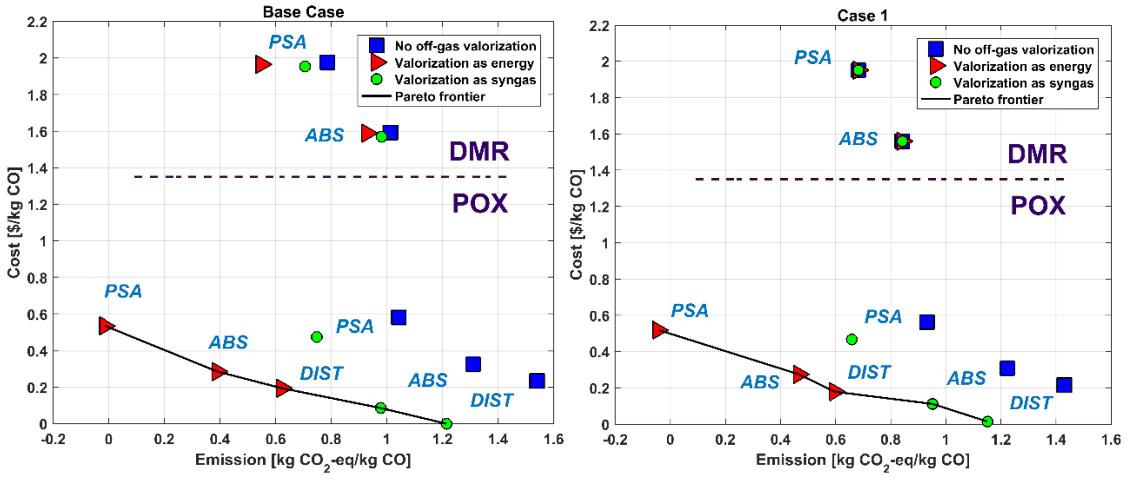

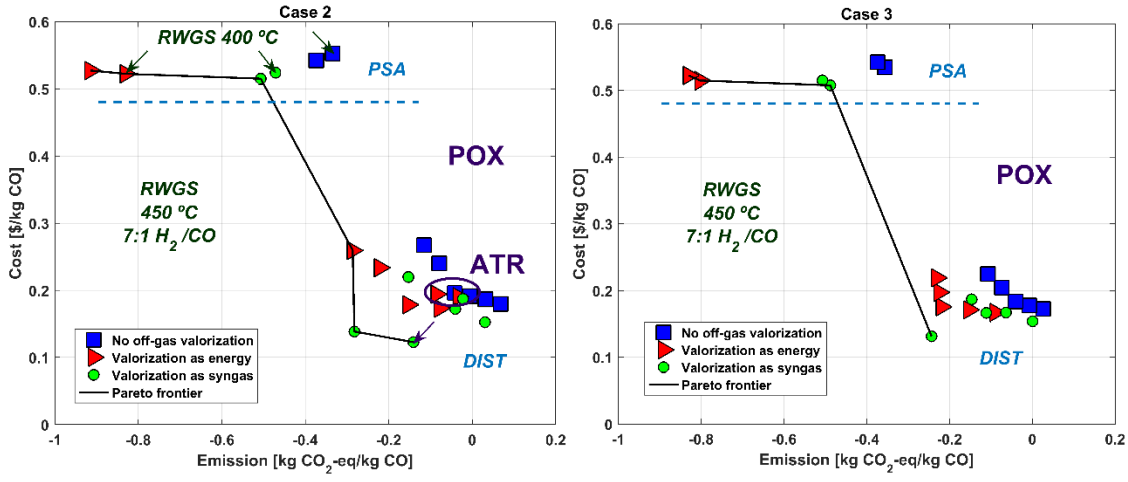

Figure 3. Results of the multi-objective optimizations of the carbon monoxide synthesis proposed model. The employed syngas synthesis and separation technologies are included along with the RWGS reactor operating conditions in the applicable case scenarios.

3.1.Base case studies (before off-gas valorization)

The minimum cost solution of the base case scenario represents the classic CO synthesis and provides a reference solution in order to compare with other non-conventional configurations. The resulting emission (1.54 kg CO_2-eq/kg) falls in the reported range (1.40 - 2.32 kg CO_2-eq/kg [10]) for CO synthesis, while the cost (0.234 $/kg) is almost within it (0.254 – 0.281 $/kg [14]), which reinforces the reliability of this result. The selected configuration consists of partial oxidation (POX) for the synthesis and cryogenic distillation as the main carbon monoxide separation technology, which matches with the most utilized syngas production and CO separation processes used industrially for this task [20,26,27,29]. This configuration is only natural since the minimum production costs sought at industrial level should be provided by the most used technologies. As the emission decreases (and the cost increases), the selected CO separation technology shifts to absorption, followed by adsorption (PSA) and when the production reaches its minimum emission values, the selected syngas synthesis process changes to Dry Methane Reforming (DMR). The emission can be decreased down to 0.786 kg CO_2-eq/kg CO (49 % reduction) but the cost rises dramatically, almost tenfold. On the one hand, the shift in separation technology can be mainly explained with each process energy demands. Absorption suffers from significant operating costs due to solvent regeneration and usage while PSA requires an elevated electricity supply in addition to its high capital cost [32]. However, neither of these technologies relies on the use of a high emitting refrigerant like cryogenic distillation does, resulting in overall less emitting processes despite the

meaningful energy requirement. On the other hand, DMR has been proven to net consume CO_2 when producing low H_2/CO syngas ratios [11], which explains its usage in the minimum emission solutions for CO synthesis, which is technically the lowest H_2/CO syngas ratio. However, the high endothermicity of its main reaction results in elevated production costs due to a significant energy demand.

Results of the inclusion of the fuel cell in Case 1 show a positive effect since both cost and emission objectives are overall moderately reduced, specially the latter. The clean electricity produced by the fuel cell undeniably reduces the emissions, however, this reduction is damped by the additional effort required to separate and achieve the fuel cell grade purity H_2. The cost, on the other hand, is barely affected in comparison to the base case. Fuel cell electricity is notorious for its higher cost compared to the traditional power plant supply, which is mainly related to the obtaining of hydrogen. In this case study, and even though it requires purification, H_2 is but a byproduct of CO production. This means that a steady supply of the gas is available without specifically synthesizing it, which is translated into a less expensive fuel cell electricity production.

As shown in Case 2 results (Figure 3), the inclusion of a RWGS reactor drastically reduces both cost and emission, even below the carbon neutrality barrier. The RWGS reaction takes advantage of the surplus H_2 and consumes CO_2 in order to form water and CO. The consequences of this are twofold: first, the high consumption of CO_2 greatly reduces the overall GWP of the process; and second, the additional CO production in the RWGS reactor reduces raw material and energy demand in the reforming section, along with their associated cost and emission. Regarding the technology selection for the synthesis, Auto-thermal Reforming (ATR) appears as one of the minimum cost solutions additionally to POX, while DMR disappears from the minimum emission solutions. POX and ATR are closely related. Not only do they use similar raw materials, produce similar

533 H_2/CO ratio syngas and possess high exothermicity but also they are the two most used
534 syngas synthesis processes precisely for this very reason. The absence of DMR in the
535 minimum emission solution is explained by the inclusion of the RWGS reactor. The
536 RWGS reaction requires H_2, however, DMR produces around half the quantity provided
537 by POX and ATR. This fact makes the latter processes more suitable to work with the
538 RWGS reactor than DMR, while the role of the CO_2 consuming process is adopted by
539 the former. The selected separation technology in the minimum cost scenario is again
540 cryogenic distillation, while the minimum emission results require PSA. Case 3 results in
541 the combination of Case 1 and 2, where the moderate reduction in cost and emission of
542 the former adds up to the high effect of the latter, in the overall best case scenario.

543 *3.2.Off-gas valorization*

544 The off-gas composition as well as the potential energy produced in its combustion
545 process are shown in Figure 4 and Figure 5, respectively. The base case scenario Pareto
546 frontier after byproduct valorization is shown in Figure 3. Valorization as syngas holds
547 the minimum cost results while the use as energy is preferred in order to achieve the
548 lowest emission values. Note that the minimum production cost after off-gas valorization
549 as syngas is close to zero. This is due to the byproduct composition being mainly H_2 with
550 barely no CO (Figure 4). It is clear that syngas and hydrogen are relevant products with
551 many applications and the manufacture of such valuable byproducts can economically
552 overshadow the main product yield. However, even if CO is theoretically less valuable
553 than H_2, its production is still mandatory in the chemical industry so as to synthesize a
554 wide range of value added products (Figure 1).

555 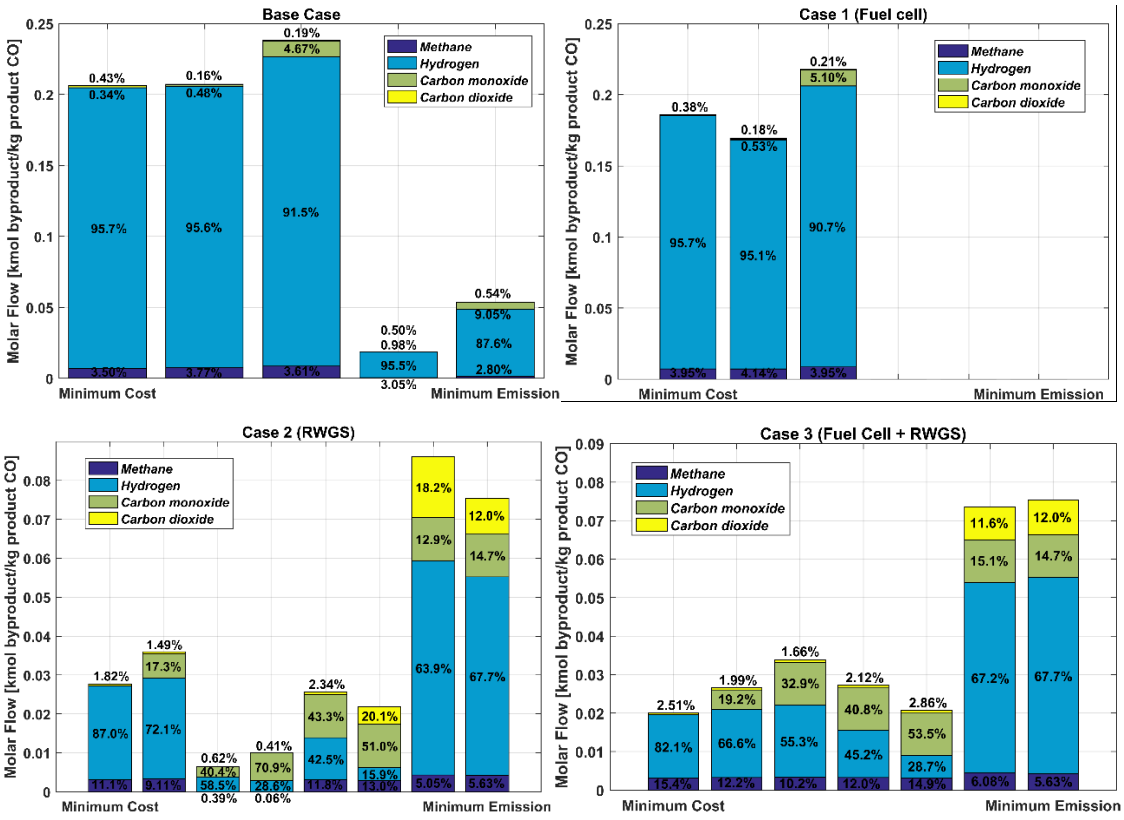

556

557 *Figure 4. Off-gas byproduct stream molar flows and compositions (Figure 3).*
558 *Compositions from bottom to top: methane, hydrogen, carbon monoxide and carbon*
559 *dioxide.*

560 This hydrogen rich off-gas has another important feature. When producing energy, the
561 associated emission is way lower than that of natural gas combustion. This translates into
562 a more than appreciable CO_2 abatement when substituting the fuel, with results slightly
563 below carbon neutrality, even though no CO_2 consumption is achieved in the related
564 process configuration. Case 1 results are again similar compared to the base case.
565 However, the most striking difference is not in the main results (Figure 3) but the in the
566 off-gas production (Figure 4), where the overall quantity of byproduct is reduced as effect
567 of the fuel cell usage due to the off-gas being mainly composed of H_2. Furthermore, this
568 reduction is increasingly marked at lower emission configurations, to the point where
569 there is no byproduct production whatsoever. This decreasing off-gas yield at minimum

emissions has yet another cause. The utilization of DMR as the reforming process vastly increases hot utility consumption in comparison with POX. Therefore, less or even no off-gas is produced due to its use as a fuel inside the system boundaries. This behavior is reflected in the energy production (Figure 5), since it is closely related to the off-gas yield.

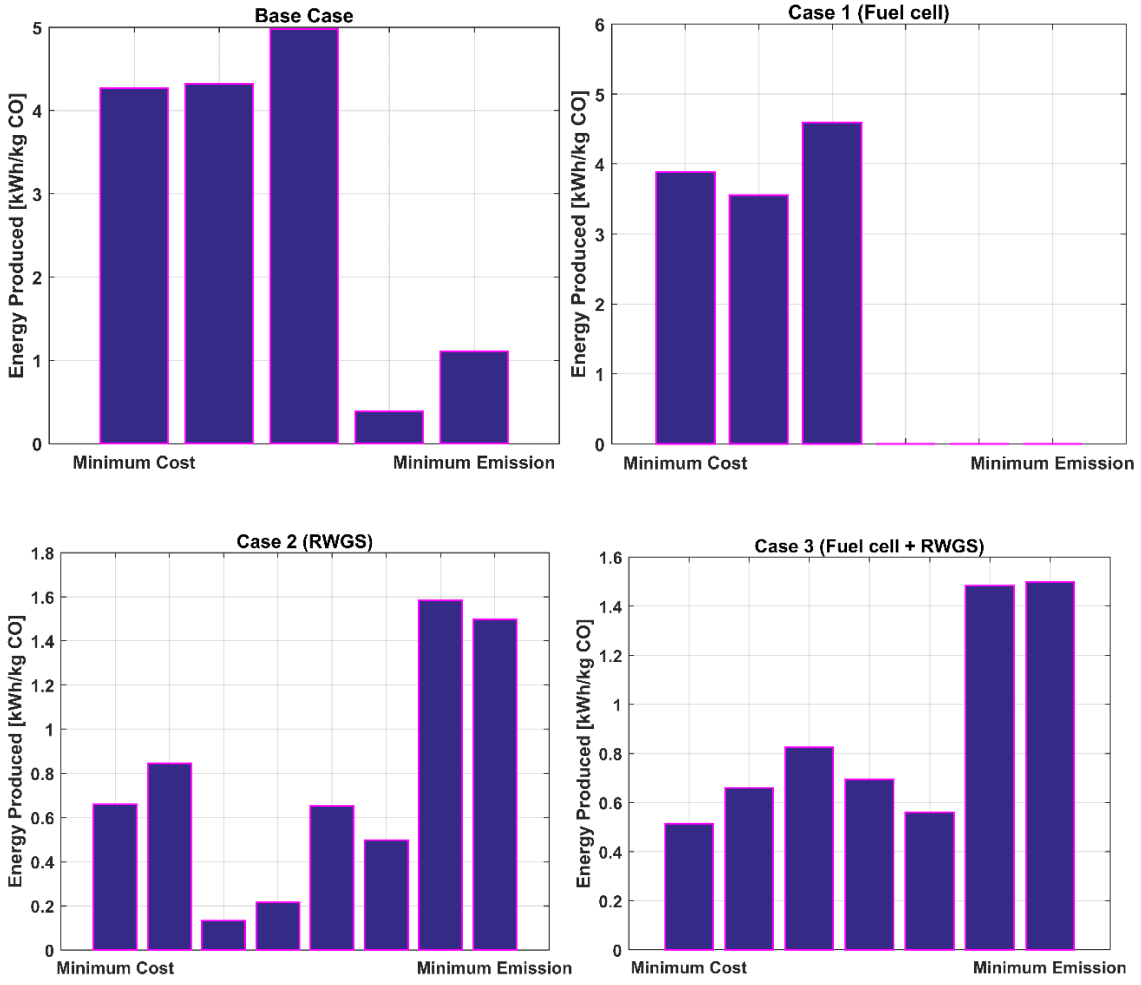

Figure 5. Energy produced when valorizing the off-gas in the synthesis of CO (Figure 3).

Although production costs after valorization are still lower in the first two case studies, results located in the Pareto frontier of Case 2 and 3 are situated well below the carbon neutrality barrier (Figure 3). Note that both the minimum cost and minimum emission solutions of Case 2 are lower than those of Case 3, even though the latter possesses the additional feature of the fuel cell that should result in the opposite. The fuel cell consumes some of the off-gas in order to produce energy, reducing the overall byproduct yield.

583 Before valorization, this extra consumption has a positive effect in both objectives,
584 however, after valorization, the reduced off-gas production is noticeable as the byproduct
585 cost and emission input is lower, resulting in slightly best cases overall when only the
586 RWGS reactor is considered (Case 2).

587 Overall off-gas compositions (Figure 4) in the first two cases where no RWGS reactor is
588 involved are hydrogen rich, with H_2/CO ratios well over 100 and only two cases being
589 slightly below 20. This off-gas can be utilized in ammonia synthesis, process that already
590 possesses a syngas to H_2 upgrading (water gas shift reaction, WGS) and CO_2/methane
591 separation system [49]. The addition of the RWGS reactor (Case 2 and 3) evens out the
592 ratios, especially in the intermediate area where cost and emission are neither minimum
593 nor maximum. Many of these ratios revolve around the value of two, which is the optimal
594 composition for methanol and Fischer-Tropsch synthesis [50,51]. This syngas would be
595 especially useful in acetic and formic acid synthesis where the raw materials needed for
596 the most relevant synthesis routes are carbon monoxide and methanol [5,7], making these
597 three processes perfectly integrable.

598 *3.3.Carbon dioxide consumption*

599 The consumption of CO_2 for the production of CO in all case studies is shown in Figure
600 6. In the first two case studies (no RWGS inclusion), the minimum cost points are situated
601 below the zero consumption mark, which is equivalent to net production of CO_2. These
602 solutions use POX (Figure 3) as their syngas reforming technology, which is not a CO_2
603 utilizing process (in fact, it is produced in the reaction). As emission decreases, CO_2
604 consumption soars to 0.8 – 0.9 kg CO_2-eq/kg, which is the consequence of using DMR
605 so as to produce syngas (Figure 3). On the other hand, when including the RWGS reactor,
606 CO_2 is consumed in all solutions, even if only POX and ATR are used in the synthesis.

Note that consumption steadily increases up to 1.1 kg CO_2-eq/kg before falling again between the range of 0.8 – 0.9 kg CO_2-eq/kg. This behavior may seem contradictory but it actually highlights a paramount matter: maximizing CO_2 consumption is not necessarily the best solution when the objective of a study is the reduction of the overall emission of a process. This is the reason why the GWP indicator, that not only considers CO_2 consumption but also indirect CO_2 emissions of other sources, is the best choice when tackling a CO_2 consumption study.

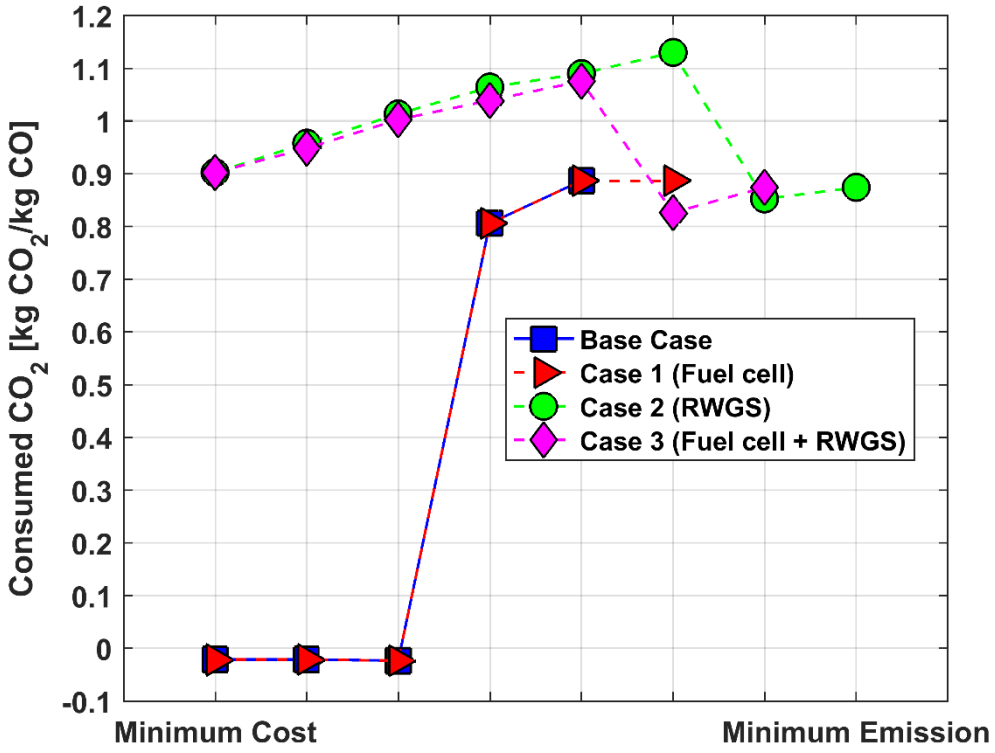

Figure 6. Carbon dioxide consumption in the synthesis of CO.

4. Conclusions

Carbon monoxide synthesis and separation is a key step in the production of many important bulk chemicals. This operation generates an off-gas byproduct which is often hydrogen rich and ends up being used as fuel. In this work, we propose a process superstructure in which different synthesis and separation technologies, alternative

hydrogen utilization pathways and the possibility of consuming CO_2 in the process of carbon monoxide synthesis are considered. The results show that the minimum cost (0.23 \$/kg CO, 1.54 kg CO_2-eq/kg CO) configuration (classic synthesis) requires partial oxidation of methane (POX) and cryogenic distillation as the carbon monoxide synthesis and separation technologies. On the other hand, when minimizing the emission, dry methane reforming (DMR) and pressure swing adsorption (PSA) are the chosen technologies, which achieve almost a 50 % reduction in GWP but increase the cost about ten times compared to the base case. The inclusion of a fuel cell as an alternative hydrogen sink reduces the overall cost and emission of the synthesis. Furthermore, adding a reverse water gas shift (RWGS) reactor that consumes H_2 and CO_2 while simultaneously producing CO, results in a drastic reduction of the GWP (up to 1.9 kg CO_2-eq reduction per kg CO compared to the base case) and cost (close to 30 % in the best case), in addition to achieving a CO_2 consumption varying between 0.8 and 1.1 kg CO_2/kg CO. The effect of byproduct valorization further improves the results. The economic objective reaches its minimum value when valorizing the byproduct as hydrogen/syngas, while emission is minimum if the off-gas is used to produce energy, long surpassing the carbon neutrality barrier (-0.83 kg CO_2-eq per kg CO).

Acknowledgements

The authors gratefully acknowledge financial support to the Spanish «Ministerio de Economía, Industria y Competitividad» under project CTQ2016-77968-C3-2-P (AEI/FEDER, UE). The authors would also like to thank «Generalitat Valenciana: Conselleria de Educación, Investigación, Cultura y Deporte» for the Ph.D grant (ACIF/2016/ 062).

Appendix A.

- Data and calculated parameters used in the optimization

  See Table A.1 - Table A. 7.

Appendix B.

- Heat integration.

  See Figure B.1 and Table B.1.

Appendix C.

- Relevant results of the multi-objective optimizations
- See Figure C.1 - Figure C.4 and Table C.1 - Table C.4

APPENDIX A

Table A.1. Raw material cost (σ_j) and emission (λ_j) parameters used in the calculations of the syngas synthesis section of the model [11].

Raw material	**Source**	σ_j **[$/kg]**	λ_j **[kg CO_2-eq/kg]** [10]
Methane	Global market (96% volume)	0.2441 [34]	0.7038
Steam	Global market (chemical industry)	0.0100 [44]	0.1830
Oxygen	Cryogenic air separation unit	0.1550 [52]	0.6304
Carbon dioxide	Amine absorption	0.0431 [35]	1.0000

Table A.2. Fixed c_{ik}^{f} and variable c_{ik}^{v} cost parameters of process unit i and type k used in Eq.(10) [11].

Unit	c_{ik}^{f} **·10^{-4} [$]**	c_{ik}^{v} **[$/capacity units]**

Compressor	10.43	172.4
Heat exchanger	1.871	59.99
Reformer furnace	48.01	67.64
Process vessel*	1.531	314.1
Fuel cell [41]	-	$7.789 \cdot 10^4$

660 *used for absorber columns, the phase separator and RWGS reactors.

661

662 *Table A.3. Process utility u cost (φ_u) and emission (θ_u) used in Eqs.*(16) *and* (17) [10].

Utility	**Source**	φ_u **[$/kWh]**	θ_u **[kg CO_2-eq/kWh]**
Natural gas	Heat production at industrial furnace	0.0092 [34]	0.2122
Cooling water	Process cooling water (30°C to 40 or 45°C)	0.0013 [44]	-
Electricity	High voltage	0.1305 [53]	0.4473

663

664 *Table A.4. Utility u consumption (a_{iu}) in process unit i and additional utility*

665 *consumption (b_i) binary parameter in process unit i used in Eqs.*(16) *and* (17).

	a_{iu} **[kWh/kmol j']**			b_i
Process unit / Utility	**Natural gas**	**Cooling water**	**Electricity**	**Additional**
Phase separator	-	-	-	-
CO_2 absorber	-	-	-	1
PSA H_2	-	-	*	-
Cryogenic distillation	-	-	-	1
CO absorber [32]	11.64	0.622	6.402	1
PSA CO	-	-	*	1
Fuel cell	-	-	-	-
RWGS1 reactor	18.90	-	-	-
RWGS2 reactor	26.00	-	-	-

RWGS3 reactor	32.96	-	-	-
RWGS4 reactor	37.29	-	-	-

*Note that the electricity consumption is calculated before the PSA units and hence it is instead included in the cost and emission of the synthesis gas generation [11]:

$$power_i = \left(\frac{\gamma}{\gamma-1}\right)\eta^{-1}R_g T\sum_j F_{ij}^{in}\left[\left(\frac{P_i}{P}\right)^{\left(\frac{\gamma}{\gamma-1}\right)}-1\right] \quad (41)$$
$$\forall i \in \{syngas\ synthesis\}$$

where $power_i$ is the electricity consumption, γ is the capacity ratio fixed at 1.5, η is the compressor efficiency fixed at 0.8, R_g is the universal gas constant in kJ/(kmol·K), T is the inlet temperature (40 ºC), P_i is the working pressure of the synthesis gas reforming technology and P is the inlet pressure of the separation technologies (30 bar).

Table A.5. Emission (ψ_i) and cost (ω_i) of additional utilities or combination of utilities in process unit i used in Eqs.(16) *and* (17).

Process unit	ω_i **[\$/kmol** j'**]**	ψ_i **[kg CO₂-eq/kmol** j'**]**
Phase separator	-	-
CO_2 absorber* [35]	1.896	0.040
PSA H_2	-	-
Cryogenic distillation*	1.991 [29]	16.44 [33]
CO absorber**	3.976 [32]	7.711 [10,32]
PSA CO***	0.271 [32]	-
Fuel cell	-	-
RWGS1 reactor	-	-
RWGS2 reactor	-	-
RWGS3 reactor	-	-
RWGS4 reactor	-	-

*total operating cost and emission of the unit

676 **solvent and absorbent cost and emission

677 ***adsorbent cost

678

679

680

681

682 *Table A.6. Separation specifications (ϕ_{ijd}) of component j in side draw d and unit i*

683 *used in Eq.*(15).

	Phase separator	CO_2 absorption	H_2 PSA
	Water	**CO_2**	**H_2 pure**
CH_4	-	-	-
H_2	-	-	0.90
CO	-	0.96	-
CO_2	-	-	-
H_2O	1.00	-	-

684

	Cryogenic distillation			CO absorption			CO PSA	
	H_2-rich	**Off-gas**	**CO**	**H_2-rich**	**Off-gas**	**CO**	**H_2-rich**	**CO**
CH_4	0.95 – 0.05	-	-	0.95 – 0.05	-	-	0.95 – 0.05	-
H_2	0.95 - 0.90	-	-	0.95 - 0.90	-	-	0.95 - 0.90	-
CO	-	-	0.90	-	-	0.99	-	0.99
CO_2	0.95 – 0.05	-	-	0.95 – 0.05	-	-	0.95 – 0.05	-
H_2O	-	-	-	-	-	-	-	-

685

686 *Table A. 7. Syngas cost and emission H_2/CO molar ratio dependence used for correlating*
687 *Eqs.*(6)-(7) [11].

H_2/CO molar ratio	Cost [$/kg]	GWP [kg CO_2-eq/kg]
0.0	0.254 [14]	1.859 [10]

1.0	0.144	0.599
1.5	0.140	0.581
2.0	0.136	0.588
2.5	0.154	0.874
<100	1.580	2.192 [10]

688

689

690

APPENDIX B

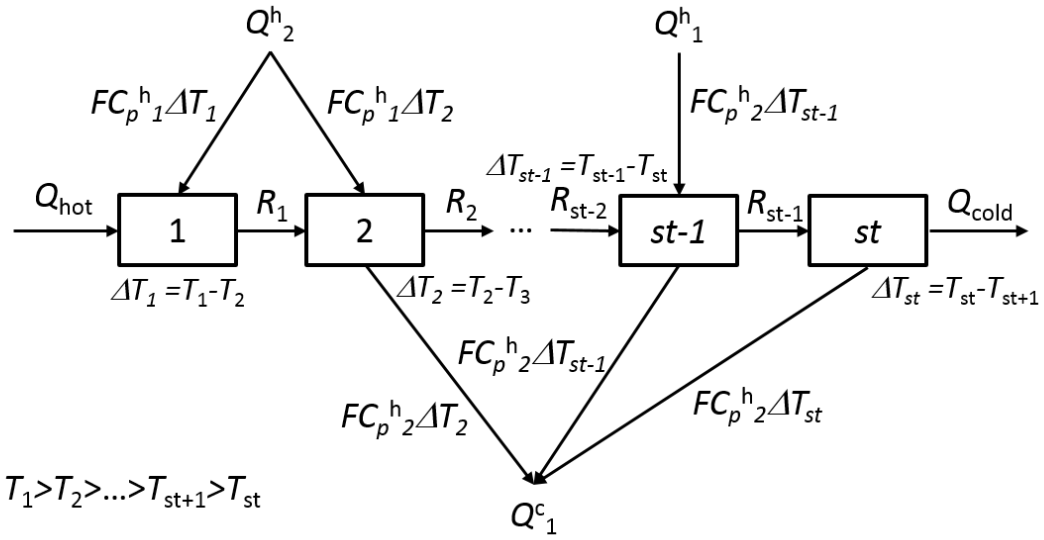

$$Q^h_1 = FC_p{}^h{}_1\Delta T^h_1 \quad \Delta T^h_2 = T_{st-1} - T_{st} = \Delta T_{st-1}$$

$$Q^h_2 = FC_p{}^h{}_2\Delta T^h_2 \quad \Delta T^c_1 = T_1 - T_3 = \Delta T_1 + \Delta T_2$$

$$Q^c_1 = FC_p{}^c{}_1\Delta T^c_1 \quad \Delta T^c_2 = T_2 - T_{st} = \Delta T_2 + ... + \Delta T_{st-1} + \Delta T_{st}$$

691

692 *Figure B.1. Transshipment problem* [45] *general example supporting the description of*
693 *section 2.4.3. Increments of temperature are taken arbitrarily.*

694

695 *Table B.1. Stream information for the transshipment problem in the proposed*
696 *superstructure (Eqs.*(25)-(27)*).*

Stream	Process	T_{in} [ºC]	T_{out} [ºC]	FC_p [kW·h/ºC·kmol j^{-1}]
h1	SMR	900	40	216
h2	POX	1197	40	99.5

Stream	Process	T_{in} [ºC]	T_{out} [ºC]	FC_p [kW·h/ºC·kmol j']
h3	ATR	1231	40	171
h4	CR	830.7	830.6	885
h5	CR	830.7	40	196
h6	DMR	850	40	129
h7	BR	850	40	193
h8	TR	827	40	271
h9	TR	827	826.9	237
h10	RWGS1	300	40	238
h11	RWGS2	350	40	238
h12	RWGS3	400	40	238
h13	RWGS4	450	40	238
c1	SMR	900	167.6	265
c2	SMR	900	899.9	1970
c3	POX	800	213.9	62.2
c4	ATR	750	151.7	160
c5	CR	850	171.4	230
c6	CR	850	849.9	1570
c7	DMR	850	40	74.5
c8	DMR	850	849.9	2460
c9	BR	850	211	138
c10	BR	850	849.9	2.2
c11	TR	827	142.8	282
c12	RWGS1	300	40	249
c13	RWGS1	300	299.9	45.8
c14	RWGS2	350	40	248
c15	RWGS2	350	349.9	176
c16	RWGS3	400	40	247
c17	RWGS3	400	399.9	300
c18	RWGS4	450	40	248

Stream	Process	T_{in} [ºC]	T_{out} [ºC]	FC_p [kW·h/ºC·kmol $j^{'}$]
c19	RWGS4	450	449.9	328

APPENDIX C

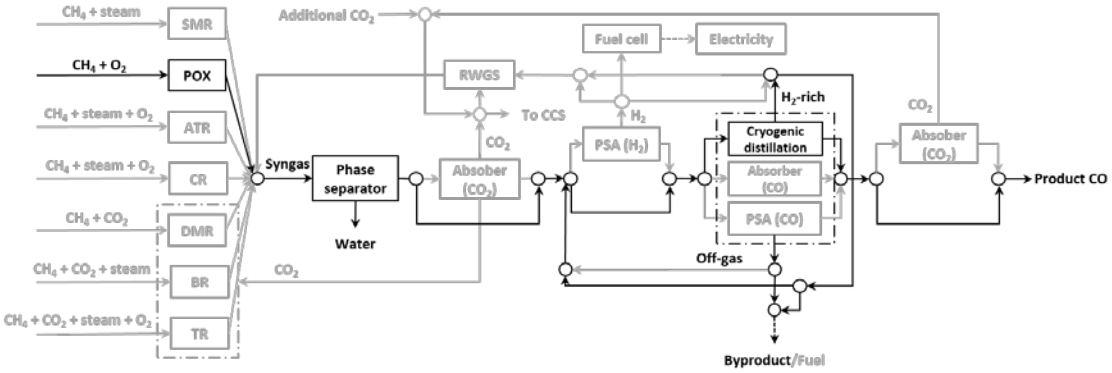

Figure C.1. Minimum cost Pareto result configuration of the Base Case multi-objective optimization (Figure 3).

Table C.1. Molar flow results [kmol/s] of Figure C.1.

	Feed	POX out	Flash out	CD in	H_2-rich	Byproduct	Product
CH_4	0.110	0.008	0.008	0.012	0.004	0.007	0.001
H_2O	-	0.006	-	-	-	-	-
O_2	0.055	-	-	-	-	-	-
CO_2	-	0.001	0.001	0.008	0.008	0.001	0.000
H_2	-	0.198	0.198	1.249	1.125	0.198	0.000
CO	-	0.101	0.101	0.111	0.011	0.001	0.100

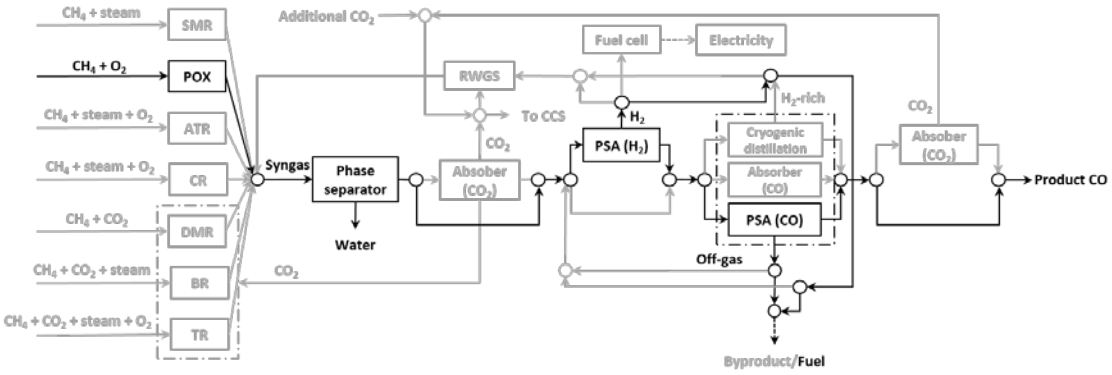

709

710 *Figure C.2. Minimum emission Pareto result configuration of the Base Case multi-*
711 *objective optimization (Figure 3).*

712

713 *Table C.2. Molar flow results [kmol/s] of Figure C.2.*

	Feed	POX out	Flash out	PSA (H_2) in	PSA (CO) in	Fuel gas	Product
CH_4	0.121	0.009	0.009	0.009	0.009	0.009	0.000
H_2O	-	0.007	-	-	-	-	-
O_2	0.061	-	-	-	-	-	-
CO_2	-	0.001	0.001	0.001	0.001	0.000	0.001
H_2	-	0.218	0.218	0.218	0.022	0.218	0.000
CO	-	0.111	0.111	0.111	0.111	0.011	0.100

714

715

716

717

718

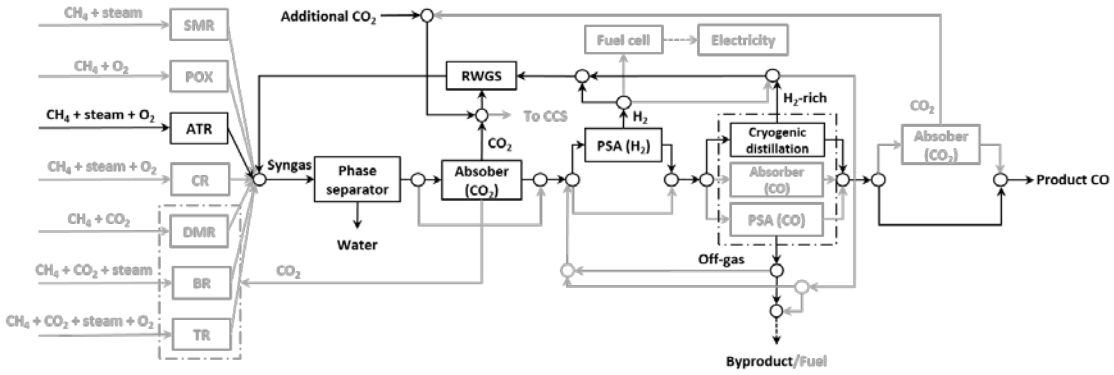

719

720 *Figure C.3. Minimum cost Pareto result configuration of Case 2 (RWGS inclusion)*

721 *multi-objective optimization (Figure 3).*

722 *Table C.3. Molar flow results [kmol/s] of Figure C.3.*

	Feed	ATR out	Flash out	PSA (H_2) in	CD in
CH_4	0.039	0.000	0.000	0.000	0.000
H_2O	0.056	0.056	0.132	-	-
O_2	0.024	-	-	-	-
CO_2	-	0.008	0.021	0.000	0.000
H_2	-	0.079	0.623	0.623	0.062
CO	-	0.031	0.111	0.111	0.111

	H_2-rich	Byproduct	RWGS in	RWGS out	Add. CO_2	Product
CH_4	0.000	0.000	0.000	0.000	-	0.000
H_2O	-	-	-	0.076	-	-
O_2	-	-	-	-	-	-
CO_2	0.001	0.000	0.089	0.012	0.088	0.001
H_2	0.059	0.003	0.620	0.543	-	0.000
CO	0.004	0.007	0.004	0.080	-	0.100

723

724

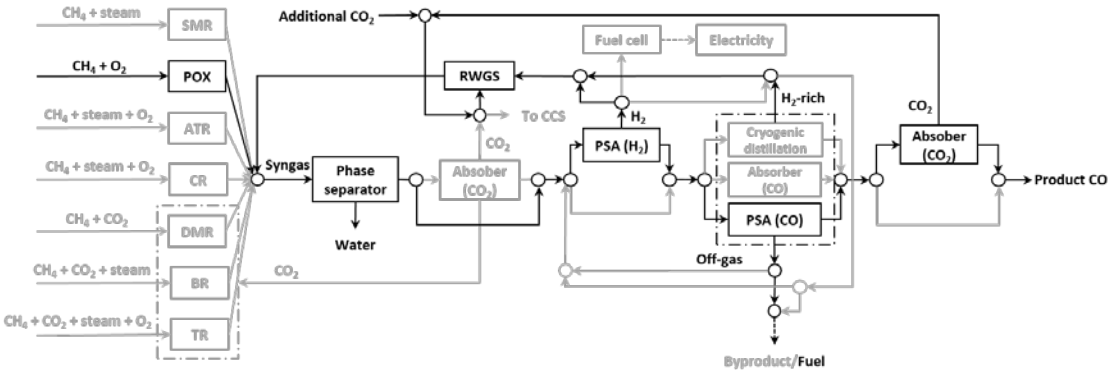

725 *Figure C.4. Minimum emission Pareto result configuration of Case 2 (RWGS inclusion)*
726 *multi-objective optimization (Figure 3).*

727 *Table C.4. Molar flow results [kmol/s] of Figure C.4.*

	Feed	POX out	Flash out	PSA (H_2) in	PSA (CO) in
CH_4	0.060	0.004	0.004	0.004	0.004
H_2O	-	0.004	-	-	-
O_2	0.060	-	-	-	-
CO_2	-	0.001	0.010	0.010	0.010
H_2	-	0.107	0.510	0.510	0.051
CO	-	0.055	0.111	0.111	0.111

	Fuel gas	RWGS in	RWGS out	Add. CO_2	Product
CH_4	0.004	0.000	0.000	-	0.000
H_2O	-	-	0.056	-	-
O_2	-	-	-	-	-
CO_2	0.009	0.066	0.009	0.066	0.001
H_2	0.051	0.459	0.403	-	0.000
CO	0.011	0.000	0.056	-	0.100

728

729

730

731

References

[1] J. Bierhals, Carbon Monoxide, in: Ullmann's Encycl. Ind. Chem., Wiley-VCH Verlag GmbH & Co. KGaA, Weinheim, Germany, 2001. doi:10.1002/14356007.a05_203.

[2] B. Cornils, W.A. Herrmann, Applied homogeneous catalysis with organometallic compounds, 1996.

[3] H. Bipp, H. Kieczka, Formamides, in: Ullmann's Encycl. Ind. Chem., Wiley-VCH Verlag GmbH & Co. KGaA, Weinheim, Germany, 2011. doi:10.1002/14356007.a12_001.pub2.

[4] M.A. Pacheco, C.L. Marshall, Review of dimethyl carbonate (DMC) manufacture and its characteristics as a fuel additive, Energy and Fuels. 11 (1997) 2–29. doi:10.1021/ef9600974.

[5] W. Reutemann, H. Kieczka, Formic Acid, in: Ullmann's Encycl. Ind. Chem., Wiley-VCH Verlag GmbH & Co. KGaA, Weinheim, Germany, 2000. doi:10.1002/14356007.a12_013.

[6] X. Yu, P.G. Pickup, Recent advances in direct formic acid fuel cells (DFAFC), J. Power Sources. 182 (2008) 124–132. doi:10.1016/j.jpowsour.2008.03.075.

[7] H. Cheung, R.S. Tanke, G.P. Torrence, Acetic Acid, in: Ullmann's Encycl. Ind. Chem., Wiley-VCH Verlag GmbH & Co. KGaA, Weinheim, Germany, 2000. doi:10.1002/14356007.a01_045.

[8] H. Held, A. Rengstl, D. Mayer, Acetic Anhydride and Mixed Fatty Acid Anhydrides, in: Ullmann's Encycl. Ind. Chem., Wiley-VCH Verlag GmbH & Co. KGaA, Weinheim, Germany, 2000. doi:10.1002/14356007.a01_065.

[9] T. Ohara, T. Sato, N. Shimizu, G. Prescher, H. Schwind, O. Weiberg, K. Marten, H. Greim, Acrylic Acid and Derivatives, in: Ullmann's Encycl. Ind. Chem.,

Wiley-VCH Verlag GmbH & Co. KGaA, Weinheim, Germany, 2003. doi:10.1002/14356007.a01_161.pub2.

[10] Ecoinvent Database 3.4, (2017). https://www.ecoinvent.org/ (accessed July 15, 2018).

[11] J.D. Medrano-García, R. Ruiz-Femenia, J.A. Caballero, Multi-objective optimization of combined synthesis gas reforming technologies, J. CO2 Util. 22 (2017) 355–373. doi:10.1016/j.jcou.2017.09.019.

[12] S. Lee, I.E. Grossmann, New algorithms for nonlinear generalized disjunctive programming, Comput. Chem. Eng. 24 (2000) 2125–2141. doi:10.1016/S0098-1354(00)00581-0.

[13] M. Ehrgott, M.M. Wiecek, Mutiobjective Programming, in: Mult. Criteria Decis. Anal. State Art Surv., Springer New York, New York, NY, 2005: pp. 667–708. doi:10.1007/0-387-23081-5_17.

[14] R. Pierantozzi, Carbon Monoxide, in: Kirk-Othmer Encycl. Chem. Technol., John Wiley & Sons, Inc., Hoboken, NJ, USA, 2000. doi:10.1002/0471238961.0301180216090518.a02.

[15] K. Aasberg-Petersen, C.S. Nielsen, I. Dybkjær, J. Perregaard, Large scale methanol production from natural gas, Haldor Topsoe. (2008) 22.

[16] A.S.K. Raju, C.S. Park, J.M. Norbeck, Synthesis gas production using steam hydrogasification and steam reforming, Fuel Process. Technol. 90 (2009) 330–336. doi:10.1016/j.fuproc.2008.09.011.

[17] R. Reimert, F. Marschner, H.-J. Renner, W. Boll, E. Supp, M. Brejc, W. Liebner, G. Schaub, Gas Production, 2. Processes, in: Ullmann's Encycl. Ind. Chem., Wiley-VCH Verlag GmbH & Co. KGaA, Weinheim, Germany, 2011. doi:10.1002/14356007.o12_o01.

[18] Hydrogen and Carbon Monoxide: Synthesis Gases, in: Ind. Gases Process., Wiley-VCH Verlag GmbH & Co. KGaA, Weinheim, Germany, n.d.: pp. 135–184. doi:10.1002/9783527621248.ch5.

[19] M.A. Peña, J.P. Gómez, J.L.G. Fierro, New catalytic routes for syngas and hydrogen production, Appl. Catal. A Gen. 144 (1996) 7–57. doi:10.1016/0926-860X(96)00108-1.

[20] E. Schwab, A. Milanov, S.A. Schunk, A. Behrens, N. Schödel, Dry reforming and reverse water gas shift: Alternatives for syngas production?, Chemie-Ingenieur-Technik. 87 (2015) 347–353. doi:10.1002/cite.201400111.

[21] X. Xiaoding, J.A. Moulijn, Mitigation of CO2by chemical conversion: Plausible chemical reactions and promising products, Energy and Fuels. 10 (1996) 305–325. doi:10.1021/ef9501511.

[22] G.A. Olah, A. Goeppert, M. Czaun, G.K.S. Prakash, Bi-reforming of methane from any source with steam and carbon dioxide exclusively to metgas (CO-2H2) for methanol and hydrocarbon synthesis, J. Am. Chem. Soc. 135 (2013) 648–650. doi:10.1021/ja311796n.

[23] S. Afzal, D. Sengupta, A. Sarkar, M. El-Halwagi, and, N. Elbashir, Optimization Approach to the Reduction of CO 2 Emissions for Syngas Production Involving Dry Reforming, ACS Sustain. Chem. Eng. 6 (2018) 7532–7544. doi:10.1021/acssuschemeng.8b00235.

[24] C. Song, Tri-reforming: A new process concept for effective conversion and utilization of CO2 in flue gas from electric power plants, ACS Div. Fuel Chem. Prepr. 45 (2000) 772–776.

[25] M. Halmann, A. Steinfeld, Fuel saving, carbon dioxide emission avoidance, and syngas production by tri-reforming of flue gases from coal- and gas-fired power

807 stations, and by the carbothermic reduction of iron oxide, Energy. 31 (2006)
808 3171–3185. doi:10.1016/j.energy.2006.03.009.
809 [26] Linde Engineering, Carbon monoxide, (2019). https://www.linde-
810 engineering.com/en/process_plants/hydrogen_and_synthesis_gas_plants/gas_pro
811 ducts/carbon_monoxide/index.html (accessed January 9, 2019).
812 [27] Pascal Marty; Arthur Darde; Antoine Hernandez;Jean-Marc Tsevery, Method for
813 simultaneously producing hydrogen and carbon monoxide, 2010.
814 [28] F. Kasuya, T. Tsuji, High purity CO gas separation by pressure swing adsorption,
815 Gas Sep. Purif. 5 (1991) 242–246. doi:10.1016/0950-4214(91)80031-Y.
816 [29] A.B. Hinchliffe, K.E. Porter, A comparison of membrane separation and
817 distillation, Chem. Eng. Res. Des. 78 (2000) 255–268.
818 doi:10.1205/026387600527121.
819 [30] N.N. Dutta, G.S. Patil, Developments in CO separation, Gas Sep. Purif. 9 (1995)
820 277–283. doi:10.1016/0950-4214(95)00011-Y.
821 [31] A.B. Hinchliffe, K.E. Porter, Gas Separation Using Membranes. 1. Optimization
822 of the Separation Process Using New Cost Parameters, Ind. Eng. Chem. Res. 36
823 (1997) 821–829. doi:10.1021/ie9603272.
824 [32] Y.-I. Lim, J. Choi, H.-M. Moon, G.-H. Kim, Techno-economic comparison of
825 absorption and adsorption processes for carbon monoxide (CO) separation from
826 linze-donawitz gas (LDG), Korean Chem. Eng. Res. 54 (2016) 320–331.
827 doi:10.9713/kcer.2016.54.3.320.
828 [33] GaBi Software and Database, (2017). http://www.gabi-software.com.
829 [34] Investing.com, (n.d.). https://www.investing.com/commodities/natural-gas
830 (accessed February 15, 2018).
831 [35] A. Nuchitprasittichai, S. Cremaschi, Optimization of CO2 capture process with

832 aqueous amines using response surface methodology, Comput. Chem. Eng. 35
833 (2011) 1521–1531. doi:10.1016/j.compchemeng.2011.03.016.
834 [36] B. Smith R J, M. Loganathan, M.S. Shantha, A Review of the Water Gas Shift
835 Reaction Kinetics, Int. J. Chem. React. Eng. 8 (2010). doi:10.2202/1542-
836 6580.2238.
837 [37] A. Wolf, A. Jess, C. Kern, Syngas Production via Reverse Water-Gas Shift
838 Reaction over a Ni-Al2O3 Catalyst: Catalyst Stability, Reaction Kinetics, and
839 Modeling, Chem. Eng. Technol. 39 (2016) 1040–1048.
840 doi:10.1002/ceat.201500548.
841 [38] B. Lu, Y. Ju, K. Kawamoto, Conversion of producer gas using NiO/SBA-15
842 obtained with different synthesis methods, Int. J. Coal Sci. Technol. 1 (2014)
843 315–320. doi:10.1007/s40789-014-0037-y.
844 [39] Y. Wang, K.S. Chen, J. Mishler, S.C. Cho, X.C. Adroher, A review of polymer
845 electrolyte membrane fuel cells: Technology, applications, and needs on
846 fundamental research, Appl. Energy. 88 (2011) 981–1007.
847 doi:10.1016/j.apenergy.2010.09.030.
848 [40] Hydrogenics, (n.d.). http://www.hydrogenics.com/hydrogen-products-
849 solutions/fuel-cell-power-systems/stationary-stand-by-power/fuel-cell-megawatt-
850 power-generation-platform/ (accessed April 15, 2018).
851 [41] Y.C. Chiang, C.T. Chang, Single-objective and multiobjective designs for
852 hydrogen networks with fuel cells, Ind. Eng. Chem. Res. 53 (2014) 6006–6020.
853 doi:10.1021/ie404068p.
854 [42] S. Sircar, T.C. Golden, Separation Science and Technology Purification of
855 Hydrogen by Pressure Swing Adsorption, (2006) 37–41. doi:10.1081/SS-
856 100100183.

[43] K. Liu, C. Song, V. Subramani, Hydrogen and Syngas Production and Purification Technologies, 2009. doi:10.1002/9780470561256.

[44] R. Turton, R.C. Bailie, W.B. Whiting, J.A. Shaeiwitz, D. Bhattacharyya, Analysis, Synthesis and Design of Chemical Processes, Fourth, Prentice Hall, 2012.

[45] S.A. Papoulias, I.E. Grossmann, A structural optimization approach in process synthesis—II: Heat recovery networks, Comput. Chem. Eng. 7 (1983) 707–721. doi:10.1016/0098-1354(83)85023-6.

[46] R. Smith, Chemical Process Design and Integration, 1994. doi:10.1529/biophysj.107.124164.

[47] GAMS Development Corporation. General Algebraic System (GAMS) Release 25.0.3. Washington, DC, USA, 2018, (n.d.).

[48] R. Misener, C.A. Floudas, ANTIGONE: Algorithms for coNTinuous / Integer Global Optimization of Nonlinear Equations, J. Glob. Optim. 59 (2014) 503–526. doi:10.1007/s10898-014-0166-2.

[49] M. Appl, Ammonia, 2. Production Processes, in: Ullmann's Encycl. Ind. Chem., Wiley-VCH Verlag GmbH & Co. KGaA, Weinheim, Germany, 2011. doi:10.1002/14356007.o02_o11.

[50] A. de Klerk, Fischer-Tropsch Process, in: Kirk-Othmer Encycl. Chem. Technol., John Wiley & Sons, Inc., Hoboken, NJ, USA, 2013. doi:10.1002/0471238961.fiscdekl.a01.

[51] A.C. Vosloo, Fischer-Tropsch: A futuristic view, Fuel Process. Technol. 71 (2001) 149–155. doi:10.1016/S0378-3820(01)00143-6.

[52] M.J. Kirschner, A. Alekseev, S. Dowy, M. Grahl, L. Jansson, P. Keil, G. Lauermann, M. Meilinger, W. Schmehl, H. Weckler, C. Windmeier, Oxygen, in:

Ullmann’s Encycl. Ind. Chem., American Cancer Society, 2017: pp. 1–32. doi:10.1002/14356007.a18_329.pub2.

[53] Eurostat Database, Electricity prices by type of user, (2017). https://ec.europa.eu/eurostat/tgm/refreshTableAction.do;jsessionid=W_AzykoJwleWzqhBFk5K4y1LOZivbHBmC4qehHPdshmkD_r5w-W0!1742705336?tab=table&plugin=1&pcode=ten00117&language=en.